Estimating the rate constant of cyclic GMP hydrolysis by activated phosphodiesterase in photoreceptors

Jürgen Reingruber
Department of Computational Biology, Ecole Normale Supérieure, 46 rue d'Ulm 75005 Paris, France.

David Holcman
Department of Applied Mathematics, Weizmann Institute of Science, Rehovot 76100, Israel and
Department of Computational Biology, Ecole Normale Supérieure, 46 rue d'Ulm 75005 Paris, France

The early steps of light response occur in the outer segment of rod and cone photoreceptor. They involve the hydrolysis of cGMP, a soluble cyclic nucleotide, that gates ionic channels located in the outer segment membrane. We shall study here the rate by which cGMP is hydrolyzed by activated phosphodiesterase (PDE). This process has been characterized experimentally by two different rate constants β_d and β_{sub}: β_d accounts for the effect of all spontaneously active PDE in the outer segment, and β_{sub} characterizes cGMP hydrolysis induced by a single light-activated PDE. So far, no attempt has been made to derive the experimental values of β_d and β_{sub} from a theoretical model, which is the goal of this work. Using a model of diffusion in the confined rod geometry, we derive analytical expressions for β_d and β_{sub} by calculating the flux of cGMP molecules to an activated PDE site. We obtain the dependency of these rate constants as a function of the outer segment geometry, the PDE activation and deactivation rates and the aqueous cGMP diffusion constant. Our formulas show good agreement with experimental measurements. Finally, we use our derivation to model the time course of the cGMP concentration in a transversally well stirred outer segment.

I. INTRODUCTION

The modern theory of chemical reactions originates back to Arrhenius [1], who showed in 1889 that the backward rate constant k_b of two reactants depends exponentially on the temperature and the activation energy barrier. However, the molecular description of the backward rate started with the seminal paper of Kramers in 1940 [2] (see also [3, 4]). The constant k_b is used to describe the chemical reaction of abundant species in solution and the concentration of the product resulting of the interaction of two molecules is calculated by using the mass action law. But, The computation also involves the forward k_f rate and the concentration of the two species. At a molecular level, k_f reflects the mean time for one of molecule to meet the other by diffusion, and the probability to react upon encounter. For diffusion limited chemical reactions, based on the mean time for a uniform concentration of particles inside an infinite 3-dimensional space to hit a sphere of radius a, von Smoluchowski obtained in 1914 the first estimate $k_f = 4\pi aD$ [5]. The Smoluchowski formula was later on extended to the case of a partially absorbing sphere [6, 7] .

Diffusion plays in many cases a prominent role in the determination of the forward binding rate [8, 9, 10, 11, 12], and numerous fundamental processes in cellular biology rely on the rate at which diffusing molecules hit a small target site: examples are trapping in patchy surfaces [13], receptor dwell time inside a synapse [14] and many more. When the number of molecules is not large, the mass action law is not sufficient to account for the random nature of the chemical reactions and other approaches are required [15]. In addition, in a confined geometry, the Smoluchowski formula does not describe the refine structure of the bounded space. For that purpose, the small hole approximation was developed, which is the mean time for a Brownian particle to escape a confined domain through a small window [15, 16, 17]. However, all these computations rely on the assumption that the reaction volume is quite homogenous and has a shape close to a convex domain (no bottle neck).

In photoreceptor outer-segment, a diffusing molecule needs to find a specific target site in a degenerated domain, where one dimensional length is much smaller than the others, and thus previous related to the small hole formula do not apply. This problem contains two difficulties: first, the target site occupies only a tiny portion of the boundary, and second, the diffusion occurs in a narrow domain.

We shall now be specific and explain what is our goal in the context of phototransduction: Rod photoreceptors are highly specialized biological devices that can detect a single photon absorption [18, 19, 20, 21]. The photon absorption activates a cascade of chemical reactions in the outer segment, which

ultimately hyperpolarizes the cell [21, 22, 23, 24, 25, 26]. The inner structure of a rod outer segment is very specific and can be considered as a cylinder that contains a densely packed stack of parallel and uniformly distributed discs (see Fig. 1). The discs divide the outer segment into almost separate compartments that are loosely connected through a narrow gap between the disc perimeters and the outer segment membrane, which we refer to as the outer shell [27]. Compartments are also linked through disc incisures, however, since their impact is small [28] we will neglect them in first approximation . The chemical reactions involved in the early steps of phototransduction occur on the surface of the internal discs, and result in the activation of the phosphodiesterase molecule (PDE) via a G-protein coupled activation cascade [21, 22, 23, 26]. A photon-excited rhodopsin activates many transducin molecules, which bind to and thereby activate PDE. The number of activated PDE molecules following a single photon absorption was studied both experimentally and theoretically [29, 30, 31, 32, 33, 34]. We refer to PDE molecules that become activated via the phototransduction cascade as light-activated PDE. In addition to the transduction pathway, PDE can also spontaneously activate, leading to a non-vanishing background activity even in darkness [30, 35].

Cytoplasmic diffusible cGMP molecules controlling the opening of cationic channels in the plasma membrane are hydrolyzed by activated PDE, and the reduction in the cGMP concentration leads to channel closure and photoreceptor hyperpolarization. From another chemical pathway catalyzed by guanyl cyclase (GC), a molecule attached to the disc surfaces and the outer segment membrane, cGMP molecules are synthesized from cytoplasmic GTP, a reaction which is calcium dependent. The magnitude of the photoresponse signal depends significantly on the number of closed ionic channels, and therefore on the drop in the cGMP concentration, which is controlled in part by the number of activated PDE and the rate of GMP hydrolysis of a single activated PDE.

cGMP hydrolysis is characterized by two rate constants β_d and β_{sub}, which are both derived from experimental measurements [22, 23, 27, 30, 33, 36, 37]. Our goal here is to derive these constants from molecular considerations and biophysical theory, and thus obtain explicit analytical expressions. To understand at an intuitive level how these rates are defined, we recall that in most photoresponse models the cGMP concentration in the outer segment is well-stirred, a simplification that neglects diffusion and the complex geometry of the outer segment. The effective differential equation for the well-stirred cGMP concentration $C(t)$ is [22, 23, 33]

$$\frac{d}{dt}C(t) = \alpha(t) - \beta_d C(t) - \beta_{sub} P_l^*(t) C(t)\,, \tag{1}$$

where $P_l^*(t)$ is the number of light-activated PDE molecules and $\alpha(t)$ the rate of cGMP synthesis. The term $\beta_d C(t)$ accounts for cGMP hydrolysis due to spontaneous PDE activation, and $\beta_{sub} P_l^*(t) C(t)$ due to light-activated PDE. Eq. 1 shows an important difference in modeling cGMP hydrolysis by spontaneously- and light-activated PDE: whereas β_d is the rate constant for the change in the cGMP concentration due to all spontaneously activated PDE in the outer segment, β_{sub} denotes the change in the well stirred cGMP concentration due to a single light-activated PDE.

In the literature, β_d and β_{sub} are considered as independent parameters, a hypothesis that is strengthened by the finding that the experimental values for β_d and β_{sub} are around $1s^{-1}$ and $10^{-4}s^{-1}$ respectively, and therefore are extremely different in appearance [22, 23, 25, 32].

Based on the diffusional encounter process between a cGMP and an activated PDE molecule in the complex rod outer segment geometry, we obtain explicit estimates for β_d and β_{sub}. Our analysis is motivated by several known results: First, in darkness, in average around one spontaneously activated PDE molecule is present in a single compartment [23, 30], which suggests that diffusion is rate limiting for hydrolysis. Second, experimental data [25, 32] indicate that activated PDE is a nearly perfect effector enzyme and hydrolyzes cGMP with a very high efficiency, which also hints that cGMP-hydrolysis is limited by diffusion. Third, a diffusion limited hydrolysis reaction couples the cytosolic cGMP level most strongly to the activation status of PDE, which is at the basis of photoreceptor adaptation [23, 38].

One of the main results of this paper is formula 32,

$$\beta_d = D_{cG} \frac{2\pi\rho\mu_+}{\mu_-} \frac{8}{4\ln(\frac{R}{a}) - 3}\,, \tag{2}$$

which relates β_d to the spontaneous PDE activation and deactivation rates μ_+ and μ_-, the PDE surface density ρ, the effective reaction radius a, the radius R of the outer segment, and the cytoplasmic cGMP

diffusion constant D_{cG}. Furthermore, by comparing this purely diffusional cGMP hydrolysis rate to experimental results, we can estimate the impact of the details of the chemical hydrolysis reaction.

The paper is organized as follows: we first determine the rate constant of cGMP hydrolysis due to a single activated PDE as a function of the cGMP concentration, the cGMP diffusion constant and the geometrical structure of the outer segment. Using this result, we then compute the analytical expressions for β_d and β_{sub}. We find that β_d is proportional to the mean number of spontaneously active PDE molecules in a compartment and not in the whole outer segment. We compare our analytical estimations with experimental measurements, and find good agreement. Our analysis suggests that the main reason for the discrepancy between β_d and β_{sub} is their incompatible definitions. By deriving β_d and β_{sub} from molecular events, we show that they are no longer two independent parameters. Finally, we use our analysis to model the spatio-temporal time course of a photoresponse in a transversally well-stirred outer segment.

II. RATE OF CGMP HYDROLYSIS BY ACTIVATED PDE

In this section, we estimate cGMP hydrolysis rate constant by a driven by single activated PDE molecule P^* when diffusion is the limiting step. Later on, we use this result to derive expressions for β_d and β_{sub}. To illustrate our approach, we start with the molecular model for cGMP hydrolysis:

$$cGMP + P^* \quad \underset{k_b}{\overset{k_f}{\rightleftarrows}} \quad cGMP{\cdot}P^* \quad \xrightarrow{k_2} \quad P^* + GMP\,. \tag{3}$$

A cGMP molecule binds to a P^* molecule with a forward rate k_f and forms an intermediate complex $cGMP{\cdot}P^*$. This complex can either dissociate with a backward rate k_b, or cGMP becomes hydrolyzed to GMP with a rate k_2. We are interested in the rate k_h by which cGMP molecules are hydrolyzed, which, at steady state, balances the $cGMP$ production rate. In the restricted rod outer segment, the overall forward binding rate is $k_f G_c$, where G_c is the number of cGMP molecules in a single compartment. As an example, in darkness, G_c is roughly in the range 100-1000, depending on the radius of the outer segment [23]. From Eq. 3, using the overall forward binding rate and Michaelis-Menton approximation, we obtain

$$k_h = \frac{k_2 k_f G_c P^*}{k_2 + k_b + k_f G_c}\,. \tag{4}$$

In the physiological range of cGMP concentrations, we assume that $k_2 \gg k_f G_c$, which implies that the hydrolysis of $cGMP{\cdot}P^*$ proceeds much faster compared to the formation of a new complex. Furthermore, since P^* hydrolyzes cGMP with very high efficiency [25, 32]), we suppose that $k_2 \gg k_b$, and therefore neglect the backward rate. Under these circumstances, Eq. 4 reduces to

$$k_h = k_f G_c P^*\,, \tag{5}$$

which has exactly the form of the hydrolysis term in Eq. 1. Eq. 5 can be formally obtained by setting $k_2 = \infty$, which means that cGMP hydrolysis occurs instantaneously after the formation of the the complex $cGMP \cdot P^*$. In contrast, if we assume that k_2 is small ($k_2 \ll k_f G_c$ and $k_b \ll k_f G_c$), using Eq. 4, this implies that hydrolysis proceeds independently of the cGMP concentration with a rate $k_2 P^*$, a scenario that is not experimentally supported [23].

For large values k_2, the cGMP hydrolysis rate in Eq. 5 is determined by the forward binding rate k_f, whose value depends on two parameters: the encounter rate k_e of cGMP molecules with the P^* site, and the probability p that $cGMP \cdot P^*$ is formed upon encounter. The probability p depends on (largely unknown) molecular properties of cGMP and activated PDE. In order to extract the impact of diffusion on cGMP hydrolysis, we set $p = 1$ and presume that the complex $cGMP \cdot P^*$ is formed each time a cGMP molecule encounters P^*. Finally, by neglecting the molecular details of activated PDE, we do not distinguish between spontaneously- and light-activated PDE, and we consider only activated versus non-activated PDE. If mainly diffusional issues are relevant for cGMP hydrolysis, then the catalytic activities of spontaneously- and light-activated PDE should be very similar, as was already suggested by experimental findings [30].

Symbol	Description
L	Length of a rod outer segment
R	Radius of a disc
d	Gap between disc and outer segment membrane
l	Distance between two adjacent disc
l_d	Width of a disc
a_P	Radius of a PDE molecule
a_{cG}	Radius of a cGMP molecule
$a = a_P + a_{cG}$	Sum of the radii of a cGMP and PDE molecule
ρ	PDE surface density
μ_+	Spontaneous PDE activation rate
μ_-	Spontaneous PDE deactivation rate

TABLE I: Description of the parameters used in the model.

Before starting the analysis, we give range values for the main parameters: cGMP diffuses in the cytosolic volume V_{cyto} of the outer segment with a diffusion coefficient $D_{cG} \approx 100\mu m^2/s^{-1}$ [35, 37, 39, 40]. In contrast, PDE molecules are attached to the disc surfaces, where they diffuse with a diffusion coefficient $D_{PDE} \approx 0.8\mu m^2/s^{-1}$ [29]. The exact geometrical dimensions of a rod outer segment varies between species [23, 41]: for example, the length L and radius $R+d$ of the outer segment in a toad rod are $60\mu m$ and $3\mu m$, whereas in a mouse rod they are $20\mu m$ resp. $3\mu m$ [23]. The longitudinal distance l between two adjacent discs (the height of a compartment) and the width of a disc l_d (see Fig. 1) vary around $15nm$ [41]. The width d of the outer shell is comparable to l [41]. The total number of compartments $N_c = \frac{L}{l+l_d}$ in the outer segment is of the order $N_c \sim 10^3$. Finally, we assume that the radii a_P of a PDE molecule and a_{cG} of a cGMP molecule are both comparable to the radius of a rhodopsin molecule, which is around 1-2nm [29]. The parameters are summarized in Table I.

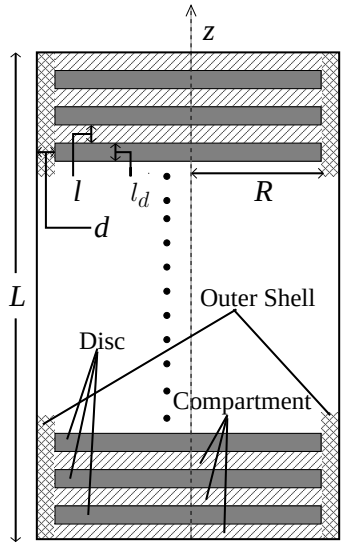

FIG. 1: Section through a cylindrical rod outer segment, containing a densely packed stack of parallel and uniformly distributed discs. The volume delimited by two adjacent discs is called a compartment.

A. Analysis of cGMP hydrolysis due to a single activated PDE

To describe the time course of cGMP concentration in the outer segment, we consider different players: cGMP molecules are independent and diffuse freely inside the outer segment domain Ω. Whenever a cGMP molecule hits the boundary area $\partial\Omega_h$ occupied by the P^* molecules, it becomes instantaneously hydrolyzed. The synthesis of cGMP occurs on the surface $\partial\Omega - \partial\Omega_h$ with a rate $\alpha_\sigma(\boldsymbol{x}, t)$. We account for these interactions by using the density $C(\boldsymbol{x}, t)$ of cGMP molecules at position $\boldsymbol{x}$ and time t, it satisfies the diffusion equation with the appropriate boundary condition [4],

$$\frac{\partial}{\partial t}C(\boldsymbol{x},t) = D_{cG}\triangle C(\boldsymbol{x},t)\,, \quad \text{for } \boldsymbol{x}\in\Omega \tag{6}$$

$$D_{cG}\frac{\partial}{\partial n}C(\boldsymbol{x},t) = -\alpha_\sigma(\boldsymbol{x},t)\,, \quad \text{for } \boldsymbol{x}\in\partial\Omega-\partial\Omega_h \tag{7}$$

$$C(\boldsymbol{x},t) = 0\,, \quad \text{for } \boldsymbol{x}\in\partial\Omega_h\,. \tag{8}$$

We shall now study Eq. 6 for a single compartment Ω_c.

Approximation of cGMP hydrolysis in a single compartment

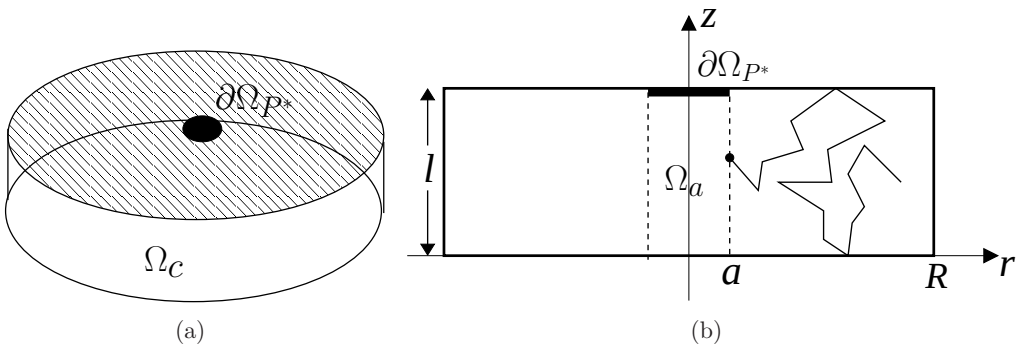

FIG. 2: (a) Elementary cylindrical compartment with a P^* molecule located centrally on the upper surface. (b) Cross-section view of the compartment. A cGMP molecule is hydrolyzed when reaching the boundary of the volume Ω_a at $r = a$.

We now consider a compartment Ω_c in which a single PDE molecule is activated on either one of the two disc surfaces (in Fig 4a P^* is attached to the upper surface). In our approximation, cGMP hydrolysis rate is given by the flux J_h of cGMP to the surface area $\partial\Omega_{P^*}$ occupied by a P^* molecule. To compute J_h, we shall make some approximations:

We consider a uniform and time independent cGMP synthesis rate α_σ. Because cGMP synthesis is calcium dependent, this corresponds to a calcium clamped outer segment or at equilibrium (this is the case in darkness). Furthermore, because the height l of a compartment is around a few nm, and much smaller compared to the radius $R \sim \mu m$, the time scale for longitudinal equilibration l^2/D_{cG} is much shorter than the one for radial equilibration $\sim R^2/D_{cG}$. Hence, newly synthesized cGMP molecules at the surface quickly equilibrate in longitudinal direction before encountering a P^* molecule, which is usually located far away compared to the compartment height l (except for the negligible amount cGMP synthesized in direct neighborhood of P^*). This scenario is equivalent to having cGMP synthesized inside the compartment, and we therefore replace cGMP synthesis on the surface by synthesis inside the volume. The volume synthesis rate α_v is linked to α_σ by

$$\alpha_v = 2\frac{\alpha_\sigma}{l}, \tag{9}$$

where the factor 2 accounts for the two disc surfaces enclosing a compartment. With a volume synthesis rate α_v, the diffusion equation for cGMP is

$$\frac{\partial}{\partial t}C(\boldsymbol{x},t) = D_{cG}\triangle C(\boldsymbol{x},t) + \alpha_v\,, \quad \text{for } \boldsymbol{x} \in \Omega_c. \tag{10}$$

The boundary conditions are given by Eq. 8 and Eq. 7 with $\alpha_\sigma(\boldsymbol{x},t) = 0$.

Because cGMP diffuses much faster than PDE ($D_{PDE} \ll D_{cG}$) we neglect PDE motion [29, 42, 43]. Since at leading order approximation the exact position of the activated PDE is not relevant [44, 45, 46], we position P^* at the center of the disc. We will discuss this issue in more detail in section III. In addition, we approximate cGMP molecules by infinitesimal points, and use the effective reaction radius $a = a_P + a_{cG}$ for a P^* molecule [29, 42, 43].

Because the effective diameter $2a \sim 6nm$ of the boundary area $\partial\Omega_{P^*}$ occupied by a P^* molecule is comparable to the compartment height $l \sim 15nm$, and the radius $R \sim 3\mu m$ is much larger than a and l, the main limiting factor for cGMP hydrolysis rate is the speed by which cGMP molecules find P^*. We note that once a cGMP molecule enters into a neighborhood of $\partial\Omega_{P^*}$, since $2a$ is comparable to l, it has a high probability to hit $\partial\Omega_{P^*}$ and become hydrolyzed. In a first approximation, we model the hydrolysis reaction by assuming that a cGMP molecule entering the small cylindrical volume Ω_a (given in cylindrical coordinates by $r \leq a$) above or below $\partial\Omega_{P^*}$ is instantaneously hydrolyzed (see Fig. 2). The corresponding boundary condition is

$$C(\boldsymbol{x},t) = 0\,, \quad \text{for } r = a\,. \tag{11}$$

This condition leads to an overestimation of the true hydrolysis rate because cGMP molecules entering the domain Ω_a can as well leave this region without touching the surface $\partial\Omega_{P^*}$. However, in appendix A, we show that the overestimation is in the range of a factor 2 (see also the discussion in section III).

Having discussed the approximations, we shall now proceed to estimate the cGMP flux J_h into $\partial\Omega_a$. We are particularly interested in J_h as a function of the cGMP concentration inside the compartment. From there, we will extract cGMP hydrolysis rate due to a single activated PDE. With this result, we will then derive the expression for β_d (see Eq. 1). Using the cylindrical symmetry, Eq. 10 reduces to

$$\frac{\partial}{\partial t}C(r,t) \;=\; D_{cG}\frac{1}{r}\frac{\partial}{\partial r}r\frac{\partial}{\partial r}C(r,t) + \alpha_v\,, \tag{12}$$

$$C(r,t) \;=\; 0 \quad \text{for } r = a\,. \tag{13}$$

Integrating Eq. 12 over the compartment volume yields an equation for the time dependent number of cGMP molecules $G_c(t)$ in Ω_c,

$$\frac{d}{dt}G_c(t) = -J_R(t) - J_h(t) + \alpha_v\pi R^2 l\left(1 - \frac{a^2}{R^2}\right)\,, \tag{14}$$

where

$$G_c(t) \;=\; 2\pi l\int_a^R C(r,t)rdr\,, \tag{15}$$

$$J_h(t) \;=\; 2\pi a l D_{cG}\frac{\partial}{\partial r}C(r,t)\Big|_{r=a}\,, \tag{16}$$

$$J_R(t) \;=\; -2\pi R l D_{cG}\frac{\partial}{\partial r}C(r,t)\Big|_{r=R}\,. \tag{17}$$

The flux $J_R(t)$ is maintained by cGMP molecules that diffuse between compartments. To derive an expression for J_h, we consider the steady state regime where the flux J_R is given. The steady state concentration $C(r)$ obtained from Eq. 12 is given by

$$C(r) \;=\; \frac{\alpha_v\pi R^2}{2\pi D_{cG}}\left(\ln\left(\frac{r}{a}\right) - \frac{r^2-a^2}{2R^2}\right) - \frac{J_R}{2\pi D_{cG}l}\ln\left(\frac{r}{a}\right)\,. \tag{18}$$

To obtain the number of G_c molecules inside a compartment, we insert Eq. 18 into Eq. 15 and for $\frac{a}{R} \ll 1$, we obtain :

$$G_c = \alpha_v \pi R^2 l \frac{R^2}{D_{cG}} \left(\frac{1}{2} \ln \left(\frac{R}{a} \right) - \frac{3}{8} \right) - J_R \frac{R^2}{D_G} \left(\frac{1}{2} \ln \left(\frac{R}{a} \right) - \frac{1}{4} \right) . \tag{19}$$

We define the times τ_1 and τ_2 and the corresponding rates k_1 and k_2 as

$$\tau_1 = \frac{1}{k_1} = \frac{R^2}{D_{cG}} \left(\frac{1}{2} \ln \left(\frac{R}{a} \right) - \frac{3}{8} \right) , \tag{20}$$

$$\tau_2 = \frac{1}{k_2} = \frac{R^2}{D_{cG}} \left(\frac{1}{2} \ln \left(\frac{R}{a} \right) - \frac{1}{4} \right) , \tag{21}$$

we can rewrite expression 19 as

$$G_c = \frac{\alpha_v \pi R^2 l}{k_1} - \frac{J_R}{k_2} . \tag{22}$$

At steady state, the value of J_h is fixed by the balance of fluxes, and Eq. 14 gives for $\frac{a}{R} \ll 1$

$$J_h = -J_R + \alpha_v \pi R^2 l . \tag{23}$$

Using Eq. 22 we can express α_v as a function G_c and J_R,

$$\alpha_v \pi R^2 l = k_1 G_c + \frac{k_1}{k_2} J_R . \tag{24}$$

Finally, inserting Eq. 24 into Eq. 23 yields

$$J_h = k_1 G_c + \frac{k_1 - k_2}{k_2} J_R . \tag{25}$$

Formula 25 gives the steady state hydrolysis rate J_h as a function of G_c and J_R. This result depends strongly on the diffusional and geometrical properties of the microdomain. Whereas Eq. 23 gives a direct expression for J_h as a function of the synthesis rate α_v, and does not involve diffusion, Eq. 25 is related to α_v indirectly via the value of G_c, and therefore involves diffusion.

In appendix A we obtain an interpretation for the two times τ_1 and τ_2, and, thus, for the rates k_1 and k_2: τ_1 (see Eq. A21) is the mean time for uniformly distributed cGMP molecules to reach the absorbing boundary at $r = a$, given reflecting boundary conditions at $r = R$; τ_2 (see Eq. A17 for $r = R$) is the mean time to reach $r = a$, when the initial position is uniformly distributed at $r = R$. In reality, there is no reflecting boundary at $r = R$, however, a vanishing flux J_R is mathematically equivalent to a reflecting boundary condition at $r = R$.

B. Derivation of the rate constant β_d for spontaneous PDE activation

In darkness, spontaneous PDE activation leads to a uniform cGMP hydrolysis in the outer segment [22, 23, 30] with an overall hydrolysis rate (see Eq. 1 integrated over the cytoplasmic volume)

$$J_{d,os} = \beta_d G_{os} , \tag{26}$$

where G_{os} is the total number of cGMP molecules in the outer segment. To derive an analytical expression for the rate constant β_d, we start from Eq. 25. Because spontaneous PDE activation occurs uniformly throughout the outer segment, apart from fluctuations, the flux J_R between compartments vanishes in darkness. Thus, the steady state hydrolysis rate J_h of a single P^* molecule given in Eq. 25 can be written as

$$J_h = k_1 G_c . \tag{27}$$

To obtain the dark hydrolysis rate $J_{d,c}$ per compartment, we have to further consider the mean number of spontaneously activated PDE molecules $P^*_{s,c}$ in a compartment. As long as the number $P^*_{s,c}$ is small and the P^* molecules are geometrically well separated [47], the rate $J_{d,c}$ increases linearly with $P^*_{s,c}$. Hence, we obtain

$$J_{d,c} = k_1 P^*_{s,c} G_c \,. \tag{28}$$

The hydrolysis rate in the whole outer segment $J_{d,os}$ is obtained by summing $J_{d,c}$ over all N_c compartments. Since $G_{os} = N_c G_c$ well approximates the total number of cGMP molecules in the outer segment (the volume $2\pi RdL$ of the outer shell is negligible compared to the volume $\pi R^2 l N_c$ of all compartments), we obtain

$$J_{d,os} = k_1 P^*_{s,c} G_{os} \,. \tag{29}$$

Finally, by comparing Eq. 29 with Eq. 26 and by using Eq. 20, we obtain

$$\beta_d = k_1 P^*_{s,c} = \frac{D_{cG}}{R^2} \frac{8}{4\ln\left(\frac{R}{a}\right) - 3} P^*_{s,c} \,. \tag{30}$$

We conclude that β_d is determined by the mean number of spontaneously activated PDE in a compartment, and not in the outer segment [30]. Furthermore, we will now relate β_d to the spontaneous PDE activation rate μ_+, the deactivation rate μ_-, and the PDE surface density ρ. The number of PDE on the disc surfaces attached to a single compartment is $P_c = 2\pi R^2 \rho$, and $P^*_{s,c}$ is given by

$$P^*_{s,c} = P_c \frac{\mu_+}{\mu_-} = 2\pi R^2 \rho \frac{\mu_+}{\mu_-} \,. \tag{31}$$

Together with Eq. 20 and Eq. 30 we obtain the final expression

$$\beta_d = D_{cG} \frac{2\pi\rho\mu_+}{\mu_-} \frac{8}{4\ln(\frac{R}{a}) - 3} \,. \tag{32}$$

C. Effective set of equations to model cGMP dynamics

By generalizing our previous results, we shall now derive an effective set of equations to model cGMP dynamics following a photon absorption. Since a photon absorbtion transiently generates an elevated amount of P^* molecules inside the affected compartment, it induces an increased cGMP hydrolysis and a cGMP gradient in the outer segment. In this case, the fluxes J_R between compartments are no longer zero after a photon absorption.

We start the derivation by extending the equilibrium expression for J_h given in Eq. 25 to time dependent situations. Because free cGMP diffusion is fast, cGMP equilibrates quickly inside a compartment. In contrast, $G_c(t)$ and $J_R(t)$ fluctuations are determined by the effective longitudinal diffusion between the compartments, which is strongly hindered by the compartmentalization of the outer segment [27, 40, 48]. Thus, we consider that $G_c(t)$ and $J_R(t)$ fluctuate on a slower time scale compared to the equilibration time scale inside a compartment. Under this condition, a first approximation of the time dependent hydrolysis rate $J_h(t)$ of a single P^* molecule is given by the equilibrium expression in Eq. 25 with time dependent $J_R(t)$ and $G_c(t)$:

$$J_h(t) = k_1 G_c(t) + \frac{k_1 - k_2}{k_2} J_R(t) \,. \tag{33}$$

We note that the expression for J_h given in Eq. 25 can be extended to time dependent cases, whereas this is not possible starting from Eq. 23.

To obtain the set of equations for the time dependent number of cGMP molecules inside a compartment, we start when a photon is absorbed in compartment n_0, while the other compartments $n = 1 \ldots N_c$, $n \neq n_0$ remain unperturbed. In the regime considered here, cGMP hydrolysis depends linearly on $P^*_l(t)$.

Using Eq. 14, the equation for the number $G_c^{(n)}(t)$ of cGMP molecules in a compartment n is given by (δ_{n,n_0} is the Kronecker-Delta)

$$\frac{d}{dt}G_c^{(n)}(t) = -J_R^{(n)}(t) - (P_{s,c}^* + P_l^*(t)\delta_{n,n_0})J_h^{(n)}(t) + \alpha_v \pi R^2 l\,. \tag{34}$$

Inserting the expression for $J_h^{(n)}(t)$ given in Eq. 33, and using the definition of β_d in Eq. 30, we obtain

$$\begin{aligned}\frac{d}{dt}G_c^{(n)}(t) \;=\; & -\left(1 + (P_{s,c}^* + P_l^*(t)\delta_{n,n_0})\frac{k_1 - k_2}{k_2}\right) J_R^{(n)}(t) \\ & -\beta_d G_c^{(n)}(t) - k_1 P_l^*(t)\delta_{n,n_0} G_c^{(n)}(t) + \alpha_v \pi R^2 l\,.\end{aligned} \tag{35}$$

By approximating the transversally well stirred cGMP concentration in a compartment by $C^{(n)}(t) \approx \frac{G_c^{(n)}(t)}{\pi R^2 l}$, and by using Fick's law, the fluxes $J_R^{(n)}(t)$ are approximated by

$$\begin{aligned}J_R^{(n)}(t) \;&=\; -D_{cG} 2\pi R d \left(\frac{C^{(n+1)}(t) - C^{(n)}(t)}{l + l_d} + \frac{C^{(n-1)}(t) - C^{(n)}(t)}{l + l_d}\right) \\ &=\; -D_{cG}\frac{2d}{Rl}\left(\frac{G_c^{(n+1)}(t) - G_c^{(n)}(t)}{l + l_d} + \frac{G_c^{(n-1)}(t) - G_c^{(n)}(t)}{l + l_d}\right)\,.\end{aligned} \tag{36}$$

Eqs. 35 and 36 constitute a close system of equations for the $G_c^{(n)}(t)$ (which can be transformed into equations for the concentrations $C^{(n)}(t)$). Furthermore, Eq. 35 models the impact of spontaneously- and light-activated PDE in an equivalent way. The simulation in Fig. 3 shows the time course of the number of cGMP molecules, scaled with respect to the dark equilibrium value, after the absorption of a photon at time $t = 0$ in the middle of the outer segment. The parameters for the simulation are suitable for a toad rod [23]. The input function $P_l^*(t)$ is obtained using the set of equations published in [34].

D. Derivation of the rate constant β_{sub} in a well stirred outer segment

We now derive an analytic expression for the rate constant β_{sub} using the approximation of a well stirred outer segment [23]. Since the volume of the outer shell is negligible compared to the combined volume of all compartments, the total number of cGMP molecules in the outer segment is

$$G_{os}(t) = \sum_{n=1}^{N_c} G_c^{(n)}(t). \tag{37}$$

By summing Eq. 35 over all compartments, and using that $\sum_{n=1}^{N_c} J_R^{(n)}(t) \approx 0$ (we neglect the cGMP molecules in the outer shell), we obtain

$$\frac{d}{dt}G_{os}(t) = -\frac{k_1 - k_2}{k_2} P_l^*(t) J_R^{(n_0)}(t) - \beta_d G_{os}(t) - k_1 P_l^*(t) G_c^{(n_0)}(t) + \alpha_v \pi R^2 l N_c\,. \tag{38}$$

In a well stirred outer segment we have $G_c^{(n)}(t) = G_{os}(t)/N_c$. By further neglecting the term $-\frac{k_1-k_2}{k_2}P_l^*(t)J_R^{(n_0)}(t)$ (the flux J_R vanishes in a well stirred outer segment), we get

$$\frac{d}{dt}G_{os}(t) = -\beta_d G_{os}(t) - \frac{k_1}{N_c} P_l^*(t) G_{os}(t) + \alpha_v \pi R^2 l N_c\,. \tag{39}$$

Finally, dividing Eq. 39 with the cytosolic volume $V_{cyto} \approx \pi R^2 l N_c$ yields the standard equation for the well stirred cGMP concentration $C(t) = G_{os}(t)/V_{cyto}$,

$$\frac{d}{dt}C(t) = -\beta_d C(t) - \frac{k_1}{N_c} P_l^*(t) C(t) + \alpha_v\,. \tag{40}$$

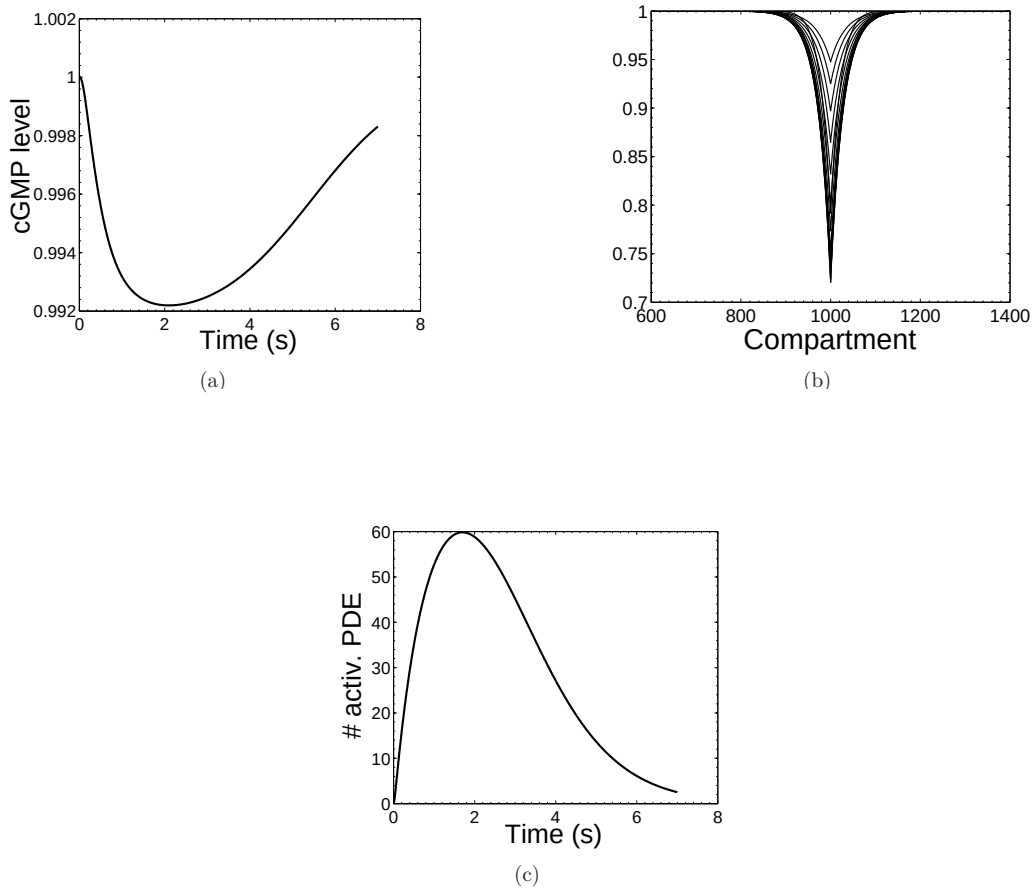

(a) (b) (c)

FIG. 3: cGMP dynamics after a photon absorption at time $t = 0$ in compartment $n = 1000$ ($N_c = 2000$). The simulation is performed using Eqs. 35 and 36. The cGMP concentration is scaled with the equilibrium value. (a) Time dependent cGMP level averaged over the outer segment. (b) cGMP level per compartment for various time points. (c) Number of light-activated PDE molecules obtained using the equations published in [34].

By comparing Eq. 40 with Eq. 1 we obtain for β_{sub} the expression

$$\beta_{sub} = \frac{k_1}{N_c} = \frac{\beta_d}{N_c \bar{P}^*_{s,c}} \,. \tag{41}$$

Since N_c is of the order 10^3, it follows that β_{sub} is much smaller than β_d. Using Eq. 20 for k_1 and $V_{cyto} \approx \pi R^2 l N_c$, Eq. 41 can be written as

$$\beta_{sub} = \frac{\pi D_{cG} l}{V_{cyto}} \frac{8}{4 \ln\left(\frac{R}{a}\right) - 3} \,. \tag{42}$$

By comparing expression 42 with the standard definition of β_{sub} given by [22, 23] (we neglect cytoplasmic buffering for cGMP [32, 37])

$$\beta_{sub} = \frac{k_{sub}}{K_m N_{Av} V_{cyto}} \,, \tag{43}$$

we obtain a new formula for $\frac{k_{sub}}{K_m}$ given by (N_{Av} is the Avogadro number)

$$\frac{k_{sub}}{K_m} = \frac{N_{Av} V_{cyto} k_1}{N_c} = \frac{8\pi D_{cG} l N_{Av}}{4\ln\left(\frac{R}{a}\right) - 3}\,. \tag{44}$$

III. COMPARISON WITH EXPERIMENTAL RESULTS

To validate our computations, we now compare our analytical results for β_d and β_{sub} (Eq. 30 and Eq. 41) with experimental measurements [23, 27, 30, 33]. We start with β_d. Using data available for toad rods, $\rho = 100\mu m^{-1}$, $R = 3\mu m$, $\mu_+ = 4 \times 10^{-4} s^{-1}$, $\mu_- = 1.8 s^{-1}$, $D_{cG} = 100\mu m^2/s^{-1}$, $a = 3nm$, $l = 15nm$ [23, 27, 30], and inserting these values into Eq. 20, Eq. 31 and Eq. 30, we obtain $k_1 = 3.6 s^{-1}$, $P^*_{s,c} = 1.26$ and

$$\beta_d = k_1 P^*_{s,c} \approx 4.5 s^{-1}\,. \tag{45}$$

This analytic result has to be compared to the experimentally found value $\beta_d \approx 1 s^{-1}$ [23], which is approximately four times smaller than this prediction. Eq. 32 shows that β_d depends only logarithmically on the compartment radius R, and thus it is very similar across species that differ mostly on the radius of the outer segment, in agreement with experimental findings [23]. The discrepancy between our theoretical prediction and the experimental value for β_d can be attributed to several factors:

1. We made the assumption that a cGMP molecule already becomes hydrolyzed when reaching the inner cylinder Ω_a at $r = a$. Thus, the time τ_1 in Eq. 20 is shorter than the true time needed to arrive at the P^* site. Hence, Eq. 20 overestimates the hydrolysis rate. In appendix A, we derive an accurate estimate for the mean time τ a cGMP molecule reaches the P^* site located on the surface of a compartment (see Eq. A23). Compared to τ_1 (Eq. 20), the new estimate for τ includes specifically the mean time τ_a a cGMP molecule starting on the boundary of Ω_a reaches the P^* molecule on the surface. By considering the additional time τ_a, we replace τ_1 and τ_2 with the more accurate expressions $\tilde{\tau}_1 = \tau_a + \tau_1$ and $\tilde{\tau}_2 = \tau_a + \tau_2$. Accordingly, the rates k_1 and k_2 have to be replaced by $\tilde{k}_1$ and $\tilde{k}_2$, given by

$$\tilde{k}_1 = \frac{1}{\tilde{\tau}_1} = \frac{1}{\tau_a + \tau_1}\,, \quad \tilde{k}_2 = \frac{1}{\tilde{\tau}_2} = \frac{1}{\tau_a + \tau_2}\,. \tag{46}$$

   For toad rod values with $l/a \sim 5$ and $R/a \sim 1000$, and by using Eq. A23 with $g(5) \approx 2.9$ (the value $g(5)$ is obtained from Fig. 5b), we find that $\tilde{k}_1 \approx 0.5 k_1$. By using $\tilde{k}_1$ instead of k_1 in Eq. 30 we obtain the new estimation

$$\beta_d = \tilde{k}_1 P^*_{s,c} = 2.25 s^{-1}\,, \tag{47}$$

   which is closer to the experimental observation.

2. Our assumption that every encounter between cGMP and P^* results in cGMP hydrolysis will certainly lead to an overestimation of the hydrolysis rate. Moreover, since we neglected the molecular details of the hydrolysis reaction, this will also induce an error. Nevertheless, since our analytic result for β_d is very close to the experimental finding, we conclude that cGMP hydrolysis by P^* has to be largely diffusion limited, and in addition has to be quite efficient, such that nearly every encounter between cGMP and activated PDE leads to a hydrolysis reaction. This is supported by the experimental observations that activated PDE hydrolyzes cGMP with very high efficiency [25, 32].

3. Uncertainties in the experimental values for D_{cG}, μ_+ and μ_-, involved in the computation of β_d, introduce ambiguities in our analytical prediction. For example, there is still considerable disagreements about the exact value of the diffusion constant D_{cG} [35, 37, 39, 40]. Furthermore, at first approximation, we used for the effective reaction radius a the sum of the molecular radii of a PDE and cGMP molecule. A more precise value for a will affect β_d in Eq. 47 mainly via τ_a, since τ_1 depends only logarithmically on a (see Eq. 32.

4. The value of β_d was computed by fixing the position of P^* at the disk center and neglecting possible fluxes between compartments. In general, spontaneous PDE activation and diffusion leads to P^* positions that are uniformly distributed over the disk surface, and different P^* positions in neighboring compartments induce small fluxes. We left open here the computation of the variance of the cGMP hydrolysis rate constant coming from random locations of $P*$ molecules. However, the P^* position should not much influence the rate constant for cGMP hydrolysis: The rate constant is determined by the MFPT of a cGMP molecule to find the P^* target. Outside a small boundary layer around P^* (the radius of the boundary layer is of the order of the reaction radius a), the leading order term of the MFPT in dimension 2 depends only logarithmically on the distance between cGMP and P^*, and in dimension 3 it is a constant [44, 45]. Hence, since almost all cGMP molecules are outside the boundary layer, the exact position of P^* is not important for their mean time to hydrolysis. We conclude that our expression for β_d should remain a valid approximation at first order, even when considering random P^* positions.

We shall now compare expressions Eqs. 41,42 for β_{sub}, and the ratio $\frac{k_{sub}}{K_m}$ (Eq. 44) with experimental measurements. Eq. 41 reveals that β_{sub} is a factor $N_c P^*_{s,c}$ smaller than β_d. Since N_c is of order 10^3 and $P^*_{s,c}$ of order $1-10$, this agrees with the experimental findings that β_{sub} is around 10^3-10^4 times smaller than β_d [23, 25]. From Eq. 44, we obtain the prediction

$$\frac{k_{sub}}{K_m} = \frac{N_{Av} V_{cyto} k_1}{N_c} \approx 9.2 \times 10^8 M^{-1} s^{-1} .$$

This estimation can be further improved by using the rate $\tilde{k}_1 = 0.5 k_1$ instead of k_1, giving

$$\frac{k_{sub}}{K_m} \approx 4.6 \times 10^8 M^{-1} s^{-1} ,$$

which has to be compared to $\frac{k_{sub}}{K_m} \approx 2.2 \times 10^8 M^{-1} s^{-1}$ obtained from experiment [32]. It is important to note that our analytic results for $\frac{k_{sub}}{K_m}$ and β_d (see Eq. 47) are both around two times larger than the experimental findings, which is an indirect confirmation of our assumption that β_d and β_{sub} (note that k_{sub}/K_m is proportional to β_{sub}) are not two independent rate constants, but can be derived from the same underlying hydrolysis reaction. Despite of the encouraging results, we would also like to indicate some difficulties related to the definition and derivation of the parameters β_{sub} and $\frac{k_{sub}}{K_m}$: First, we extracted the formula for $\frac{k_{sub}}{K_m}$ using the expression for β_{sub} given in Eq. 42. This approach is problematic because the definition of β_{sub} involves the assumption of a well stirred cGMP concentration during a photoresponse, which is not very accurate (see Fig. 3 and [27, 37]). Second, if diffusion limits the rate of cGMP hydrolysis in the physiological range, the experimentally observed value for $\frac{k_{sub}}{K_m}$ does not reflect an intrinsic property of the chemical reaction. Instead, it depends strongly on diffusional and geometrical details, and, therefore, on the experimental setup. For example, measurements of the Michaelis constant K_m were performed using fragments of disrupted rod outer segments with a length only a fraction of the intact outer segment length [32, 49]. Eq. 40 shows that the rate of cGMP hydrolysis increases with decreasing fragment length L (since $N_c \sim L$). Thus, the apparent value of the Michaelis constant K_m (k_{sub} is assumed to be a true constant) that is needed to fit the rate of cGMP hydrolysis will be higher in a suspension containing large fragments compared to a suspension with small fragments, as it has been observed [32, 49].

In this work we have assumed that cGMP hydrolysis in the physiological range is diffusion limited, and is independent of whether PDE is spontaneously- or light-activated. The agreement between our theoretical results and experimental measurements indicates that the large disparity between β_{sub} and β_d is largely due to their definition, and not due to biochemical differences. For example, in [27] the effect of spontaneously- and light-activated PDE was modeled using two very different rates $k = 0.042 \mu M^{-1} s^{-1}$ and $k^* = 110 \mu M^{-1} s^{-1}$. We will show now that the large discrepancy between k and k^* in [27] essentially originates from modeling needs. Indeed, cGMP hydrolysis by spontaneously activated PDE was modeled as $k[PDE]_\sigma[cGMP]$, where $[PDE]_\sigma$ is the surface concentration of PDE. In contrast, hydrolysis by light-activated PDE was modeled as $k^*[PDE^*]_\sigma[cGMP]$, with $[PDE^*]_\sigma$ as the surface concentration of light-activated PDE. By introducing the mean surface concentration of spontaneously activated PDE, $[PDE^*_s]_\sigma = [PDE]_\sigma \frac{\mu_+}{\mu_-}$, we rewrite $k[PDE]_\sigma[cGMP]$ as $k\frac{\mu_-}{\mu_+}[PDE^*_s]_\sigma[cGMP]$, which now has the same

form as $k^*[PDE^*]_\sigma[cGMP]$. Inserting the values $\mu_+ = 4 \times 10^{-4} s^{-1}$ and $\mu_- = 1.8 s^{-1}$ found in [30], we obtain $k\frac{\mu_-}{\mu_+} = 189 \mu M^{-1} s^{-1}$, which is now comparable to $k^* = 110 \mu M^{-1} s^{-1}$. We conclude that modeling cGMP hydrolysis by spontaneously- and light-activated PDE in a similar way involves comparable parameters, indicating that hydrolysis may be indeed independent of whether PDE is spontaneously- or light-activated.

IV. CGMP HYDROLYSIS IN CONES

After having discussed in detail cGMP hydrolysis in rods, we now briefly explore hydrolysis in cones. Similar to [48], our analysis for rods can be adapted to cones. Unlike rods, cones do not contain disc in the outer segment. However, the membrane invaginations in cones can be modeled similarly to discs in rods. Since the radius of the cone outer segment decreases from the bottom versus the top, we can adapt our formulas to cones by replacing the disc radius R with a compartment dependent radius R_n. Thus, in cones, the rates $\tilde{k}_1$ and $\tilde{k}_2$ depend on the compartment n. Therefore, the response to a photon absorption in cones varies on the location where the photon has been absorbed. Since $k_1 P^*_{s,c}$ depends logarithmically on the compartment radius R_n (see Eq. 30), we suggest that the value for the dark hydrolysis rate β_d in cones should be of the same magnitude as found in rods, see also [35].

V. SUMMARY AND DISCUSSION

In this paper, we have studied the rate constant of cGMP hydrolysis by activated PDE in rod and cone photoreceptors. Our analysis is based on the assumption that cGMP hydrolysis is diffusion limited and determined by the encounter rate between cGMP and activated PDE. We derived an explicit formula for the rate constant of cGMP hydrolysis by a single activated PDE molecule as a function of the confined outer segment geometry and the cGMP diffusion constant (Eq. 27). Our calculation takes into account the complex structure of the rod outer segment, uniformly divided by a stack of parallel discs into homogenous microdomains, called compartments, and coupled to each other via cGMP diffusion. We obtained analytical expressions for the rate constants β_d and β_{sub}. In addition, we give a set of effective equations that allow to model the transversally well stirred cGMP concentration after a photon absorption.

Interestingly, we found that only the amount of spontaneously activated PDE in a single compartment is needed to calculate the dark hydrolysis rate β_d (see Eq. 30). This result differs from [30], where the compartmentalization was not considered, and all spontaneously activated PDE in the outer segment additively contribute to β_d. Because the number of spontaneously activated PDE in the outer segment is by a factor $N_c \sim 10^3$ larger compared to a single compartment, the catalytic activity of an excited PDE in [30] was estimated much lower compared to what we found here. We computed the PDE activity (given by the rate $\tilde{k}_1$ in Eq. 46) to be around $1 s^{-1}$, whereas in [30] it is around $10^{-5} s^{-1}$. Using the rates for spontaneous PDE activation and deactivation [30], we estimate that the average number of spontaneously activated PDE molecules in a single compartment is around one. Together with our result for the PDE activity, this naturally explains the experimental value $\beta_d \sim 1 s^{-1}$. For the derivation of β_d, it was essential to assume that cGMP hydrolysis occurs locally at the activated PDE site. In contrast, if cGMP hydrolysis occurred uniformly over the disc surface, then the experimental value for β_d could not be recovered without introducing additional adjusting parameters (see appendix B).

We have derived a set of equations (Eqs. 35 and 36) that allow to calculate the time course of the transversally well stirred cGMP concentration following a photon absorption. These equations model cGMP hydrolysis by spontaneously and light-activated PDE in a similar way. Under the assumption that cGMP concentration in the outer segment is well stirred, we derived an expression for the rate β_{sub} (Eq. 41,42), and the ratio $\frac{k_{sub}}{K_m}$ (Eq. 44).

Eq. 41 connects β_{sub} to β_d and gives a direct explanation why β_{sub} is found to be so much smaller than β_d. Our result suggests that the large discrepancy between β_d and β_{sub} is largely due to their definitions: β_d incorporates the effect of all spontaneously activated PDE in the outer segment, while β_{sub} accounts for only a single light-activated PDE.

APPENDIX

APPENDIX A: MEAN TIME TO HYDROLYSIS IN A COMPARTMENT

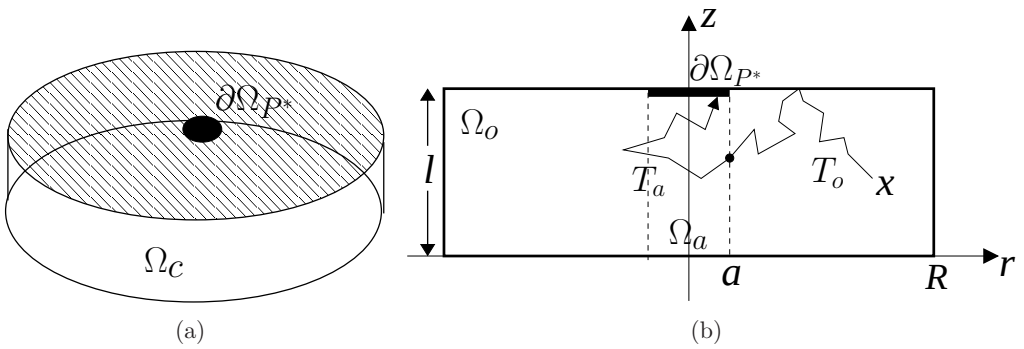

FIG. 4: (a) Cylindrical compartment Ω_c with an activated PDE molecule located centrally on the upper surface. (b) The first time a cGMP molecule hits $\partial\Omega_{P^*}$, when starting at position $\boldsymbol{x}$ in Ω_o, is given by the sum of two times. First, the time T_o for a molecule starting at $\boldsymbol{x}$ to arrive at the boundary $\partial\Omega_a$, and second, the time T_a for the particle starting at $\partial\Omega_a$ to arrive at $\partial\Omega_{P^*}$.

In this part of the appendix, we shall obtain a precise estimate for the mean time τ a cGMP molecule starting uniformly distributed inside the cylindrical compartment Ω_c reaches the activated PDE molecule, defined as the small surface patch $\partial\Omega_{P^*}$ with radius $r = a$ (see Fig 4). The motion of the cGMP molecule is Brownian in Ω_c. It is reflected all over the boundary except at $\partial\Omega_{P^*}$, where is is absorbed. We denote by $T^{(x)}$ the random initial time a cGMP molecule starting at $\boldsymbol{x} \in \Omega_c$ hits $\partial\Omega_{P^*}$. Due to rotational invariance, the Mean First Passage Time (MFPT) $\tau(\boldsymbol{x}) = \mathrm{E}[T^{(x)}|\boldsymbol{x}(0) = \boldsymbol{x}]$ depends only on r and z. Using a cylindrical coordinate system $\boldsymbol{x} = (r, \varphi, z))$, we decompose the domain Ω_c into the inner cylinder

$$\Omega_a = \{\boldsymbol{x} \in \Omega_c | r \leq a\}\,, \tag{A1}$$

and the hollow cylinder

$$\Omega_o = \Omega_c - \Omega_a = \{\boldsymbol{x} | a \leq r \leq R\}. \tag{A2}$$

We define the mean time τ as the average over a uniform initial distribution in Ω_c,

$$\tau = \frac{1}{|\Omega_c|}\int_{\Omega_c} \tau(r,z)dV\,. \tag{A3}$$

Using that $\Omega_c = \Omega_o + \Omega_a$, we can rewrite Eq. A3 as

$$\begin{aligned}\tau &= \frac{|\Omega_c| - |\Omega_a|}{|\Omega_c|}\frac{1}{|\Omega_o|}\int_{\Omega_o}\tau(r,z)dV + \frac{|\Omega_c| - |\Omega_o|}{|\Omega_c|}\frac{1}{|\Omega_a|}\int_{\Omega_a}\tau(r,z)dV \\ &= \frac{1}{|\Omega_o|}\int_{\Omega_o}\tau(r,z)dV - \frac{|\Omega_a|}{|\Omega_c|}\left(\frac{1}{|\Omega_o|}\int_{\Omega_o}\tau(r,z)dV - \frac{1}{|\Omega_a|}\int_{\Omega_a}\tau(r,z)dV\right)\,,\end{aligned} \tag{A4}$$

where $\frac{1}{|\Omega_o|}\int_{\Omega_o}\tau(r,z)dV$ is the mean time for particles starting uniformly distributed in Ω_o to hit $\partial\Omega_{P^*}$, and $\frac{1}{|\Omega_a|}\int_{\Omega_a}\tau(r,z)dV$ is the mean time to hit $\partial\Omega_{P^*}$ for particles starting uniformly distributed in Ω_a. Because particles originating from Ω_o have to reach Ω_a before hitting $\partial\Omega_{P^*}$, it is plausible (and can also be shown) that the mean time to $\partial\Omega_{P^*}$ for particles starting uniformly in Ω_o is larger than the mean time for particles starting uniformly in Ω_a. Furthermore, for $a \ll R$, we have $|\Omega_a| \ll |\Omega_c|$. From this, we finally obtain

$$\tau = \frac{1}{|\Omega_c|}\int_{\Omega_c}\tau(r,z)dV \approx \frac{1}{|\Omega_o|}\int_{\Omega_o}\tau(r,z)dV\,. \tag{A5}$$

Thus, for $a \ll R$, the mean time τ is well approximated by the mean time for particles starting uniformly in Ω_o to hit $\partial\Omega_{P^*}$.

We shall now estimate $\tau(r,z)$, by considering the equation [4, 50]

$$\begin{aligned} D_{cG}\left(\frac{\partial^2}{\partial r^2}+\frac{1}{r}\frac{\partial}{\partial r}+\frac{\partial^2}{\partial z^2}\right)\tau(r,z)\,, &= -1 \quad 0<z<l\,, 0\le r<R \\ \tau(r,z) &= 0\,, \quad z=l\,, r<a \\ \frac{\partial}{\partial z}\tau(r,z) &= 0\,, \quad z=l\,, r>a \\ \frac{\partial}{\partial z}\tau(r,z) &= 0\,, \quad z=0 \\ \frac{\partial}{\partial r}\tau(r,z) &= 0\,, \quad r=R\,. \end{aligned} \tag{A6}$$

We will first estimate the average time

$$\tau(r)=\frac{1}{l}\int_0^l \tau(r,z)dz\,. \tag{A7}$$

Using the dimensionless variables

$$x=\frac{r}{a}\,, \quad y=\frac{z}{a}\,, \quad \hat{\tau}(x,y)=\frac{D_{cG}}{R^2}\tau(r,z)\,, \quad \alpha=\frac{a}{R}\,, \quad \beta=\frac{l}{a}, \quad x_\alpha=\frac{1}{\alpha}\,, \tag{A8}$$

equation A6 becomes

$$\begin{aligned} \left(\frac{1}{x}\frac{\partial}{\partial x}x\frac{\partial}{\partial x}+\frac{\partial^2}{\partial y^2}\right)\hat{\tau}(x,y) &= -\alpha^2\,, \quad 0<y<\beta\,, 0\le x<x_\alpha \\ \hat{\tau}(x,y) &= 0\,, \quad y=\beta\,, x<1 \\ \frac{\partial}{\partial y}\hat{\tau}(x,y) &= 0\,, \quad y=\beta\,, x>1 \\ \frac{\partial}{\partial y}\hat{\tau}(x,y) &= 0\,, \quad y=0 \\ \frac{\partial}{\partial x}\hat{\tau}(x,y) &= 0\,, \quad x=x_\alpha\,, \end{aligned} \tag{A9}$$

and Eq. A7

$$\hat{\tau}(x)=\frac{1}{\beta}\int_0^\beta \hat{\tau}(x,y)dy\,. \tag{A10}$$

We integrate Eq. A9 over the variable y to derive an equation for $\hat{\tau}(x)$ for $x \ge 1$. Taking into account the boundary conditions at $y=0$ and $y=\beta$, we obtain

$$\begin{aligned} \frac{1}{x}\frac{\partial}{\partial x}x\frac{\partial}{\partial x}\hat{\tau}(x) &= -\alpha^2\,, \quad x>1 \\ \frac{\partial}{\partial x}\hat{\tau}(x) &= 0 \quad \text{for } x=x_\alpha \end{aligned} \tag{A11}$$

The solution is given

$$\hat{\tau}(x)=f(\alpha,\beta)+\frac{1}{2}\ln(x)-\frac{1}{4}\alpha^2(x^2-1)\,, \tag{A12}$$

with

$$f(\alpha,\beta)=\hat{\tau}(1)=\frac{1}{\beta}\int_0^\beta \hat{\tau}(1,y)dy\,. \tag{A13}$$

Hence, for $r \geq a$, we have

$$\tau(r) = \frac{R^2}{D_{cG}} f(\alpha,\beta) + \frac{R^2}{D_{cG}} \left(\frac{1}{2}\ln(x) - \frac{1}{4}\alpha^2(x^2-1) \right) \tag{A14}$$

$$= \tau_a + \tau_o(r)\,, \tag{A15}$$

where we defined

$$\tau_a = \frac{R^2}{D_{cG}} f(\alpha,\beta)\,, \tag{A16}$$

$$\tau_o(r) = \frac{R^2}{D_{cG}} \left(\frac{1}{2}\ln\left(\frac{r}{a}\right) - \frac{1}{4}\frac{r^2-a^2}{R^2} \right)\,. \tag{A17}$$

Eq. A14 has an intuitive interpretation: the mean time $\tau(r)$ for a cGMP molecule, uniformly distributed at $r > a$, is the sum of the mean time $\tau_o(r)$ to the boundary $r = a$ plus the mean time τ_a from the surface $\partial\Omega_a$ to go to $\partial\Omega_{P^*}$ (see Fig 4).

By averaging over a uniform initial distribution $\rho = \frac{1}{\pi(R^2-a^2)}$ in Ω_o, the overall mean time τ in Eq. A5 is given by

$$\tau = \frac{1}{|\Omega_o|}\int_{\Omega_o} \tau(r,z)dV = 2\pi\rho \int \tau(r) r dr$$

$$= \frac{R^2}{D_{cG}} f(\alpha,\beta) + \frac{R^2}{8D_{cG}} \frac{-4\ln(\alpha) - 3 + 4\alpha^2 - \alpha^4}{1-\alpha^2} \tag{A18}$$

$$= \tau_a + \tau_o\,, \tag{A19}$$

where we defined τ_o as

$$\tau_o = 2\pi\rho \int \tau_o(r) r dr = \frac{R^2}{8D_{cG}} \frac{-4\ln(\alpha) - 3 + 4\alpha^2 - \alpha^4}{1-\alpha^2}. \tag{A20}$$

The leading order expansion of τ_o for $\alpha \ll 1$ is

$$\tau_o = \frac{R^2}{D_{cG}} \left(\frac{1}{2}\ln\left(\frac{R}{a}\right) - \frac{3}{8} \right)\,. \tag{A21}$$

For $\alpha \ll 1$ (see also Fig. 5b), we can approximate $f(\alpha,\beta)$ by $f(0,\beta) = g(\beta)$ and obtain ($\beta = \frac{l}{a}$)

$$\tau_a \approx \frac{R^2}{D_{cG}} g\left(\frac{l}{a}\right)\,, \quad \alpha \ll 1\,. \tag{A22}$$

Altogether, for $\alpha \ll 1$, the mean time τ in Eq. A5 is given by

$$\tau = \tau_a + \tau_o \approx \frac{R^2}{D_{cG}} \left[g\left(\frac{l}{a}\right) + \frac{1}{2}\ln\left(\frac{R}{a}\right) - \frac{3}{8} \right]\,. \tag{A23}$$

To derive an explicit expression for $f(\alpha,\beta)$ and $g(\beta)$ is a difficult mathematical problem. Nonetheless, we shall obtain some asymptotic limits for $f(\alpha,\beta)$. For $\beta \to 0$ (corresponding to $l \to 0$), we have $\tau_a \to 0$, and therefore $f(\alpha,0) = 0$. For $\beta \to \infty$, the time τ_a diverges to infinity, and $f(\alpha,\beta) \to \infty$. For $a = R$, corresponding to $\alpha = 1$, we have $\tau_a = \frac{l^2}{3D_{cG}}$, from which it follows that

$$f(1,\beta) = \frac{\beta^2}{3}\,. \tag{A24}$$

Finally, the small hole theory [44] predicts that when $l \sim R \ll a$ (which implies that $\alpha \sim \beta$), the mean time τ is asymptotically given by

$$\tau \approx \frac{V}{4D_{cG}a} = \frac{\pi R^2}{4D_{cG}}\beta\,. \tag{A25}$$

By comparing Eq. A25 with Eq. A23 ($\ln(\alpha)$ can be neglected compared to β for $\alpha \sim \beta$), we obtain the asymptotic

$$g(\beta) \sim \frac{\pi}{4}\beta\,, \quad \beta \gg 1. \tag{A26}$$

So far, we have only an asymptotic expansion for $\beta \gg 1$. To explore a much larger parameter space, we decided to run Brownian simulations (10000 cGMP molecules are initially uniformly distributed over the lateral surface of $\partial\Omega_a$) to estimate τ_a and $f(\alpha, \beta)$. The numerical results for $f(\alpha, \beta)$ are summarized in Fig. 5. Fig. 5b shows that $f(\alpha, \beta)$ can be well approximated by $f(0, \beta) = g(\beta)$ for $\alpha \lesssim 0.05$.

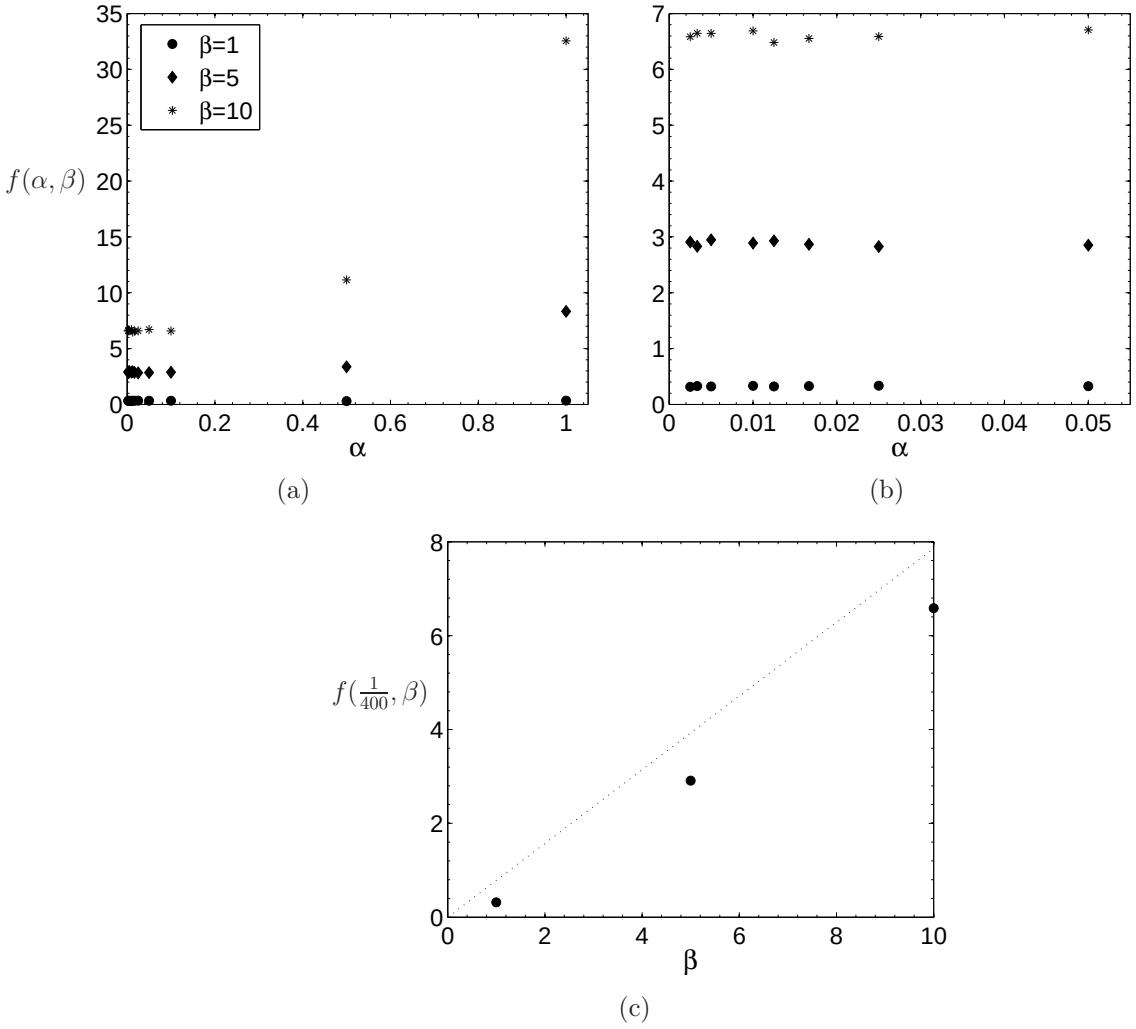

FIG. 5: Numerical evaluation of the function $f(\alpha, \beta)$ ($\alpha = a/R$ and $\beta = l/a$). Each data point is obtained using the Brownian simulation of 10000 cGMP molecules. (a) $f(\alpha, \beta)$ for different values α and β. For $\alpha = 1$ we have $f(1, \beta) = \frac{\beta^2}{3}$ (Eq. A24). (b) Same data as in (a), restricted to small α. (c) Plot of $f(\frac{1}{400}, \beta) \approx g(\beta)$ (same data as in (a) and (b)). The dashed curve represents the asymptotic $\frac{\pi}{4}\beta$ (Eq. A26), achieved for $\alpha \to 0$ and $\beta \to \infty$. For values $\beta \leq 10$ used in the simulations, the behavior of $g(\beta)$ is close, but not yet in full agreement with $\frac{\pi}{4}\beta$.

APPENDIX B: MODEL WITH UNIFORM HYDROLYSIS ON THE DISC SURFACES

In this section, we consider a model that is based on cGMP hydrolysis occurring uniformly on the disc surface (see also [27, 37]). This is very different from the situation presented within the main body of the paper, where we assumed that cGMP hydrolysis occurs locally at the P^* site. We show now that uniform cGMP hydrolysis leads to a dark rate constant proportional to $D_{cG}/l^2 \sim 10^5 s^{-1}$, which is very different from Eq. 30 (see also section III). Thus, in order to account for the experimental value $\beta_d \sim 1 s^{-1}$, one is forced to introduce a small adapting parameter κ_h.

We will analyze two different scenarios: In one situation, synthesis and hydrolysis of cGMP are both modelled by boundary source terms. In another, only hydrolysis is modelled by a boundary source term, while synthesis occurs uniformly within the cytoplasmic volume.

1. Model with boundary source terms for hydrolysis and synthesis

The reaction-diffusion equation for cGMP concentration $C(z, r, t)$ inside a compartment is given by

$$\frac{\partial}{\partial t} C(z,r,t) = D_{cG} \Delta C(z,r,t)\,, \tag{B1}$$

$$-D_{cG} \frac{\partial C(z,r,t)}{\partial z}\Big|_{\substack{z=0\\z=l}} = -\kappa_h C(z,r,t)\Big|_{\substack{z=0\\z=l}} + \alpha_\sigma(t) \tag{B2}$$

$$D_{cG} \frac{\partial C(z,r,t)}{\partial r}\Big|_{r=R} = 0 \tag{B3}$$

The steady state expressions for the concentration C of Eq. B1 and the hydrolysis rate J_h are ($G_c = \pi R^2 C$)

$$C = \frac{\alpha_\sigma}{\kappa_h}\,, \tag{B4}$$

$$J_h = 2\pi R^2 \kappa_h C = 2\frac{\kappa_h}{l} G_c\,. \tag{B5}$$

Because hydrolysis and synthesis are both modelled by fluxes originating from the same boundary, the equilibrium only reflects the balance of the fluxes, and does not involve cGMP diffusion.

2. Model with boundary source term for hydrolysis, and a volume synthesis rate

To include cGMP diffusion (see section II A), we now model cGMP synthesis by a uniform volume production rate $\alpha_v(t) = 2\alpha_\sigma(t)/l$. This model avoids the problems arising when cGMP synthesis and hydrolysis are both modelled by surface fluxes originating from the same boundary. The equation for the cGMP concentration reads

$$\frac{\partial}{\partial t} C(z,r,t) = D_{cG} \Delta C(z,r,t) + \alpha_v(t)\,, \tag{B6}$$

$$-D_{cG} \frac{\partial C(z,r,t)}{\partial z}\Big|_{\substack{z=0\\z=l}} = -\kappa_h C(z,r,t)\Big|_{\substack{z=0\\z=l}} \tag{B7}$$

$$D_{cG} \frac{\partial C(z,r,t)}{\partial r}\Big|_{r=R} = 0 \tag{B8}$$

The steady state solution of Eq. B6 is

$$C(z) = \frac{\hat{C}}{2}\frac{z}{l}(1 - \frac{z}{l}) + \frac{\hat{C}}{2\beta}\,, \tag{B9}$$

where we introduced the parameter β and the concentration $\hat{C}$ as

$$\beta = \frac{\kappa_h l}{D_{cG}}\,, \quad \hat{C} = \alpha_v \frac{l^2}{D_{cG}}\,. \tag{B10}$$

At equilibrium, the number of cGMP molecules G_c and the hydrolysis rate J_h in a compartment are

$$G_c = \pi R^2 \int_0^l C(z)dz = \hat{C}\left(\frac{1}{12}+\frac{1}{2\beta}\right)\pi R^2 l\,, \tag{B11}$$

$$J_h = \pi R^2 D_{cG}\left(\frac{dC(z)}{dz}|_{z=0} - \frac{dC(z)}{dz}|_{z=1}\right) = \pi R^2 l \alpha_v$$
$$= \frac{D_{cG}}{l^2}\left(\frac{1}{12}+\frac{1}{2\beta}\right)^{-1} G_c\,. \tag{B12}$$

Contrary to Eq. B5, the flux J_h in Eq. B12 depends on cGMP diffusion constant. In the limit $\beta \to \infty$ ($\kappa_h \to \infty$) (perfectly absorbing boundaries), we obtain $J_h = G_c/\tau$, where $\tau = \frac{l^2}{12 D_{cG}}$ is the mean time for a molecule to reach the boundaries at $z = l$ or $z = 0$. On the other hand, in the limit $\beta \to 0$, we obtain $J_h = \frac{D_{cG}}{l^2} 2\beta G_c = 2\frac{\kappa_h}{l} G_c$. Thus, we recover the expression given in Eq. B5.

Eq. B12 is formally equivalent to Eq. 27, however, the physical content is very different. J_h in Eq. B12 is proportional to the rate by which cGMP molecules collide with the disc surfaces, which is of the order $D_{cG}/l^2 \sim 10^5 s^{-1}$. In contrast, J_h in Eq. 27 is determined by the rate by which cGMP molecules find P^*, given by $D_{cG}/R^2 \sim 1 s^{-1}$. In order to obtain $\beta_d \sim 1 s^{-1}$ from Eq. B12, one needs a small value for the adapting parameter κ_h.

Acknowledgments

The authors would like to thank Maria Corado for carefully reading the manuscript. J.R. thanks the FRM-foundation for support.

[1] S. Arrhenius, Z. Phys. Chem. **4**, 226 (1889).
[2] H. A. Kramers, Physica (Amsterdam) **7**, 284 (1940).
[3] P. Hänggi, P. Talkner, and M. Borkovec, Rev. Mod. Physics **62**, 251 (1990).
[4] Z. Schuss, *Theory and Applications of Stochastic Differential Equations* (Wiley Series in Probability and Statistics, John Wiley Sons, Inc., New York, 1980).
[5] M. von Smoluchowski, Wien Berlin **123**, 12381 (1914).
[6] H. C. Berg and M. Purcell, Biophys. J. **20**, 193 (1977).
[7] R. Zwanzig, Proc. Natl. Acad. Sci. USA **87**, 5856 (1990).
[8] A. Szabo, K. Schulten, and Z. Schulten, J. Chem. Phys. **72**, 4350 (1980).
[9] K. Schulten, Z. Schulten, and A. Szabo, J. Chem. Phys. **72**, 4426 (1981).
[10] A. Perico and M. Battezzati, J. Chem. Phys. **75**, 4430 (1981).
[11] G. Wilemski and M. Fixman, J. Chem. Phys. **58**, 4009 (1973).
[12] F. C. Collins and G. E. Kimball, J. Colloid Sci. **4**, 425 (1949).
[13] A. M. Berezhkovskii, Y. A. Makhnovskii, M. I. Monine, V. Y. Zitserman, and S. Y. Shvartsman, J. Chem. Phys. **121**, 11390 (2004).
[14] A. Taflia and D. Holcman, J. Chem. Phys. **126**, 23407 (2007).
[15] D. Holcman and Z. Schuss, J. Chemical Physics **122**, 114710 (2005).
[16] I. V. Grigoriev, Y. A. Makhnovskii, A. M. Berezhkovskii, and V. Y. Zitserman, J. Chem. Phys. **116**, 9574 (2002).
[17] Z. Schuss, A. Singer, and D. Holcman, Proc. Natl. Acad. Sci. USA **104**, 16098 (2007).
[18] S. Hecht, S. Shlaer, and M. Pirenne, J. Gen. Physiol. **25**, 819 (1942).
[19] B. Sakitt, J. Physiol. **223**, 131 (1972).
[20] D. Baylor, T. Lamb, and K.-W. Yau, J. Physiol. **288**, 613 (1979).
[21] F. Rieke and D. Baylor, Rev. of Mod. Phys. **70** (1998).
[22] E. Pugh Jr and T. Lamb, Biochim. et Biophys. Acta **1141**, 111 (1993).
[23] E. Pugh Jr and T. Lamb, Handbook of Biological Physics **3** (2000).
[24] M. Burns and D. Baylor, Annu. Rev. Neurosci. **24**, 779 (2001).
[25] V. Arshavsky, T. Lamb, and E. Pugh Jr, Annu. Rev. Physiol. **64**, 153 (2002).
[26] M. Burns and V. Arshavsky, Neuron **48**, 387 (2005).

[27] D. Andreucci, P. Bisegna, G. Caruso, H. Hamm, and E. DiBenedetto, Biophys. J. **85**, 1358 (2003).
[28] G. Caruso, P. Bisegna, L. Shen, D. Andreucci, H. Hamm, and E. DiBenedetto, Biophys. J. **91**, 1192 (2006).
[29] E. Pugh Jr and T. Lamb, J. Physiol. **449**, 719 (1992).
[30] F. Rieke and D. Baylor, Biophys. J. **71**, 2553 (1996).
[31] S. Felber, H. Breuer, F. Petruccione, J. Honerkamp, and K. Hofmann, Biophys. J. **71**, 3051 (1996).
[32] I. Leskov, V. Klenchin, J. Handy, G. Whitlock, V. Govardovskii, M. Bownds, T. Lamb, E. Pugh Jr, and V. Arshavsky, Neuron **27**, 525 (2000).
[33] R. Hamer, S. Nicholas, D. Tranchina, P. Liebman, and T. Lamb, J. Gen. Physiol. **122**, 419 (2003).
[34] J. Reingruber and D. Holcman, Biophys. J. **94**, 1954 (2008).
[35] D. Holcman and J. Korenbrot, J. Gen. Physiol. **125**, 641 (2005).
[36] R. Hamer, S. Nicholas, D. Tranchina, T. Lamb, and J. Jarvinen, Vis. Neurosci. **22**, 417 (2005).
[37] G. Caruso, H. Khanal, V. Alexiadis, F. Rieke, H. Hamm, and E. DiBenedetto, IEE proc.-Syst. Biol. **153**, 119 (2005).
[38] G. Fain, H. Matthews, M. Cornwall, and Y. Koutalos, Physiological Reviews **81** (2001).
[39] Y. Koutalos, K. Nakatani, and K.-W. Yau, Biophys. J. **68**, 373 (1995).
[40] A. Olson and E. Pugh Jr, Biophys. J. **65**, 1335 (1993).
[41] S. Nickell, P. S.-H. Park, W. Baumeister, and K. Palczewski, J. of Cell Biol. **177**, 917 (2007).
[42] K. R. Naqvi, Chemical Physics Letters **28**, 280 (1974).
[43] D. C. Torney and H. M. McConnell, Proc. of the Royal Society A **387**, 147 (1983).
[44] A. Singer, Z. Schuss, D. Holcman, and B. Eisenberg, J. Stat. Phys. **122**, 437 (2006).
[45] A. Singer, Z. Schuss, D. Holcman, and B. Eisenberg, J. Stat. Phys. **122**, 465 (2006).
[46] A. Singer, Z. Schuss, and D. Holcman, J. Stat. Phys. **122**, 491 (2006).
[47] D. Holcman and Z. Schuss, J. Phys. A: Math. Theor. **41**, 155001 (2008).
[48] D. Holcman and J. Korenbrot, Biophys. J. **86**, 2566 (2004).
[49] C. Dumke, V. Arshavsky, P. Calvert, M. Bownds, and E. PUGH Jr, J. Gen. Physiol. **103**, 1071 (1994).
[50] C. Gardiner, *Handbook of Stochastic Methods* (Springer, 2003), 3rd ed.